COMPRESSIVE SAMPLING VS. CONVENTIONAL IMAGING

Jarvis Haupt and Robert Nowak

University of Wisconsin - Madison
Department of Electrical and Computer Engineering
1415 Engineering Drive, Madison, WI 53706
jdhaupt@wisc.edu, nowak@engr.wisc.edu

ABSTRACT

Compressive sampling (CS), or "Compressed Sensing," has recently generated a tremendous amount of excitement in the image processing community. CS involves taking a relatively small number of non-traditional samples in the form of randomized projections that are capable of capturing the most salient information in an image. If the image being sampled is compressible in a certain basis (e.g., wavelet), then under noiseless conditions the image can be much more accurately recovered from random projections than from pixel samples. However, the performance of CS can degrade markedly in the presence of noise. In this paper, we compare CS to conventional imaging by considering a canonical class of piecewise smooth image models. Our conclusion is that CS can be advantageous in noisy imaging problems if the underlying image is highly compressible or if the SNR is sufficiently large.

Index Terms— Image sampling, random projections

1. INTRODUCTION

Compressive Sampling (CS), or "Compressed Sensing," has recently generated a tremendous amount of excitement in the image processing community. CS involves taking a relatively small number of non-traditional samples in the form of projections of the signal onto random basis elements or random vectors (random projections). Recent results show that such observations can contain most of the salient information in the signal. It follows that if a signal is compressible in some basis, then a very accurate reconstruction can be obtained from these observations [1, 2, 3]. Our own work shows that compressible signals can be accurately recovered, at the usual nonparametric rates, from random projections that are also contaminated with zero-mean additive noise [4]. In noiseless settings, CS reconstructions are much more accurate than reconstructions obtained from an equivalent number of conventional point samples, illustrating the utility of CS.

The main contribution of this work is examination of the feasibility of CS as an imaging method through a careful comparison of its performance with more standard (pixel-based) sampling schemes. The remainder of the paper is organized as follows. In Section 2 we define the imaging problem being considered. Section 3 gives an overview of the known performance results of CS, in terms of the average squared error rates. Section 4 describes the class of images being considered. The performance of CS relative to conventional methods is predicted theoretically in Section 5. An example is presented in Section 6 and conclusions are given in Section 7.

This work was supported by the National Science Foundation, grant nos. CCR-0310889 and CNS-0519824.

2. PROBLEM STATEMENT

The imaging problem being considered is described as follows. Let $f^* = f^*(x,y),\ x,y = 1,\ldots,\sqrt{n}$, be an image defined on an n-point uniform Cartesian grid on $[0,1]^2$ where n is a perfect square. For the sake of notational simplicity, we will consider f^* as a vector (perhaps a raster-scanned representation of the original) and write $f^* = f^*_i,\ i = 1,\ldots,n$. The goal is to sample f^* and obtain a reconstruction, denoted $\widehat{f} = \widehat{f}_i,\ i = 1,\ldots,n$, that minimizes the average mean squared reconstruction error given by

$$\mathbb{E}\left[\frac{\|f^* - \widehat{f}\|_2^2}{n}\right] = \mathbb{E}\left[\frac{\sum_{i=1}^n (f^*_i - \widehat{f}_i)^2}{n}\right],$$

where the expectation is over the distribution on the noise (if present) and/or randomization of the sampling process, as described below. Note that this goal is non-trivial in the presence of noise and/or when the number of samples taken is smaller than the number of pixels.

In this paper we are interested in reconstruction from $k \ll n$ samples. First consider the problem in a noiseless setting, and a general form of sampling defined by

$$y_j = \sum_{i=1}^n \phi_{j,i} f^*_i,\ \ j = 1,\ldots,k,$$

where $\phi_{j,i}$ are *projection vectors*, chosen a priori and nonadaptively by the user, and satisfying the energy constraint $\sum_{i=1}^n \phi_{j,i}^2 = \|\phi_j\|_2^2 = 1$. For example, choosing $\phi_{j,i} = 1$ for some index i and $\phi_{j,i} = 0$ for all other indices is equivalent

to the j^{th} observation being a point or pixel sample of f^*. Many other possible sampling schemes are possible within this framework, including the randomized patterns discussed in the next section. In noisy imaging environments, the observation model changes slightly. Noisy observations are

$$y_j \;=\; \sum_{i=1}^{n} \phi_{j,i} f_i^* \;+\; w_j, \;\; j = 1, \ldots, k, \qquad (1)$$

where the w_j represent errors in the sampling process. In this paper, we assume that $w_j,\ j = 1, \ldots, k$, are i.i.d. zero-mean Gaussian noises with variance σ^2.

3. COMPRESSED SENSING THEORY

In Section 2 we defined a general form of sampling that can be used to describe many classical sampling schemes. The key to the success of Compressed Sensing (CS) is to employ random, white-noise projection vectors. This approach, coupled with tractable reconstruction algorithms, can lead to amazing results for signals that are compressible. The basic intuition behind CS is that each white-noise projection spreads its energy (in expectation) over the entire signal space, effectively "illuminating" the entire signal. But more is true. Roughly speaking, it turns out that k white-noise projections simultaneously sample all possible k-dimensional signal subspaces with high probability. Image reconstructions from white-noise samples are based on the idea of finding a reconstruction that fits the samples and also has a sparse representation in a good approximating basis. We state some formal consequences of this remarkable result below and refer the reader to the existing literature for further details [1, 2, 3, 4, 5].

Suppose that the image f^* is well approximated in a certain representation in the following sense. Let $f^{*(m)}$ denote the best m-term approximation of f^* in terms of this representation (e.g., an orthonormal basis). Suppose that the squared approximation error behaves like

$$\frac{\|f^* - f^{*(m)}\|_2^2}{n} \leq C_{\text{A}}\, m^{-2\alpha} \qquad (2)$$

for some $\alpha \geq 0$ and number $C_{\text{A}} \geq 0$ that is a constant or logarithmic (in m) factor. The parameter α quantifies the degree to which f^* is compressible in the given representation. We say that the approximation error scales as $m^{-2\alpha}$ if a relationship like the one in (2) holds. Throughout the paper, in our inequalities we will focus on the polynomial behavior and constants or logarithmic factors (like $\log m$, $\log n$, $\log k$) will be absorbed into a common factor out front.

With respect to the choice of representation, it is clear that any m-term or m-component reconstruction of f^* will exhibit a worst-case reconstruction error no better than the approximation error rate for the optimal m-term approximation. Remarkably, in noiseless conditions CS performs almost as well the optimal approximation. Specifically, suppose the $\phi_{j,i}$ are generated as i.i.d. Rademacher random variables ($\pm 1/\sqrt{n}$ each with probability $1/2$). Sampling using vectors of this form will be called *Rademacher sampling*. It can be shown that k Rademacher samples combined with a linear programming reconstruction technique based on a good approximating basis produces a reconstruction $\widehat{f}^k$ satisfying

$$\mathbb{E}\left[\frac{\|\widehat{f}^k - f^*\|_2^2}{n}\right] \leq C_{\text{CS}}\, k^{-2\alpha}$$

where $C_{\text{CS}} > 0$ includes a logarithmic factor. These results were developed in [1, 2, 3]. Note that the error decays at the same rate as the optimal k-term approximation.

When noise is present in the measurements, as described by the observation model in (1), existing bounds suggest that the reconstruction error rate degrades. A reconstruction from k noisy Rademacher samples combined with an mixed l_2-l_0 (squared data-fitting error plus l_0-norm of coefficients in the approximating basis) reconstruction criterion produces a reconstruction satisfying the error bound

$$\mathbb{E}\left[\frac{\|\widehat{f}^k - f^*\|_2^2}{n}\right] \leq C_{\text{NCS}}\, k^{\frac{-2\alpha}{2\alpha+1}}$$

as shown in [4], where again $C_{\text{NCS}} > 0$ includes a logarithmic factor. Alternatively, one can arrive at similar results via a reconstruction based on linear programming [5]. Note that the error decay can be much slower in the noisy case. Nonetheless, it is easy to see that CS can still impressively outperform conventional pixel sampling by considering an image with a very small number of non-zero pixels at arbitrary locations [4]. In this case, undersampling in the pixel domain will probably miss most of these pixels leading to an very large error, whereas the CS error decays as shown above.

4. PIECEWISE CONSTANT IMAGE CLASS

In order for CS to be a viable option, it should offer some provable advantage over classical imaging methods in more general situations. To this end, we compare the theoretical performance of CS to classical pixel-sampling for piecewise constant images. Specifically, we consider the class of images composed of constant regions separated by one-dimensional boundary curves (edges). Results similar to those stated below also hold for more general piecewise smooth images, provided the images are sufficiently smooth away from the boundaries. However, to keep the presentation and analysis simple, we work with the piecewise constant class.

The defining feature of the piecewise constant class is the following. If the image domain is partitioned into m squares of equal size, then the boundary curve (edges) occupy no more than $C\sqrt{m}$ of the squares for some constant $C > 0$ (i.e., the curve is one-dimensional). We will also consider the special subclass of images whose boundary curves are pixelized versions of twice-continuously differentiable functions.

Images in this class are compressible using a number of compressing bases or representations. The best m-term pixel or Fourier approximation of a given image in this class has a squared approximation error that scales as $m^{-1/2}$ (we will discuss the pixel approximation error in a bit of detail below). Wavelets provide a more compact representation of images in this class, yielding an approximation error that scales as m^{-1} [6, 7]. The improved rate can be attributed to the fact that an optimal dyadic wavelet partition can be chosen such that the boundary is tiled with small dyadic squares of sidelength m^{-1} and so that the total number of dyadic squares is no more than some small constant multiple of m [8, 7]. If we consider the subclass of images with twice-continuously differentiable boundary curves, then it is know that wedgelets [8], curvelets [6], and contourlets [9] yield an approximation error that scales like m^{-2}. This improvement is possible because these more sophisticated representations essentially provide a piecewise linear approximation to the boundary, leveraging the additional smoothness of the curves.

Let us examine the approximation capabilities of conventional pixel sampling in a bit more detail. Consider taking k pixel samples of the original image, where the samples are arranged on a uniform Cartesian grid of dimension $\sqrt{k} \times \sqrt{k}$ (k is a perfect square). The n-pixel reconstruction will have to be formed by "upsampling" the k-pixel subimage back to an n-pixel image. Note that in the vicinity of the boundary there is no guaranteed local smoothness or regularity between pixels. Thus, a reasonable upsampling method is to simply fill regions of the n-pixel reconstruction with the value of the nearest sampled pixel. The reconstruction will then consist of k square cells each with area $1/k$. The boundary will pass through on the order of $\sqrt{k}$ of these cells, and the reconstruction will have $O(1)$ error in each of these "boundary" cells. Therefore approximation error of this method scales as $k^{-1/2}$.

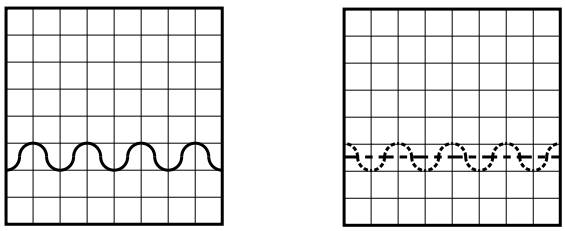

(a) True Boundary (b) Other Candidates

Fig. 1. Potential failures of cell average samples.

Another common form of image acquisition is based on integration pixel samples. In this situation, the image is partitioned into k square cells and the average is computed over each cell. On one hand, it might seem that integration sampling provides more information than pure pixel (point) samples. However, the images in Fig. 1 show that this is not the case in this image class. Fig. 1(a) depicts the boundary of an image in the class being considered, along with the partition cells corresponding to the integration sampling process. In cells containing the boundary, samples will be approximately $1/2$ assuming the constant portions on either side of the boundary are of 0 and 1, respectively. Many reconstructions other than the true boundary are consistent with the observed data (e.g., a horizontal line or a shifted version of the true boundary, as shown in Fig. 1(b)). The two alternate reconstructions will exhibit $O(1)$ error on the boundary cells, and will lead to an approximation error rate that scales as $k^{-1/2}$ by the above argument.

5. RECONSTRUCTION ERROR COMPARISON

We are now in the position to compare CS with pixel sampling for the piecewise constant image class. First let us consider pixel sampling. In the noiseless case, we obviously get the approximation rate $k^{-1/2}$. The approximation error places an upper bound on the reconstruction error that is attainable when noise is present. If the pixel samples described above are denoised using *any* method, the reconstruction error can be no better than $k^{-1/2}$.

Now consider CS. In noiseless CS, the reconstructions achieve the approximation error rates dictated by the compressing basis or representation scaling like $k^{-2\alpha}$ while in noisy settings the reconstruction error bound scales like $k^{\frac{-2\alpha}{2\alpha+1}}$, as reviewed in Section 3. The approximation rates reviewed in Section 4 show that for the piecewise constant image class, wavelet, wedgelet and curvelet approximations all yield $\alpha = 1/2$. In the subclass of piecewise constant images with smoother boundaries (twice-continuously differentiable), then wedgelets, curvelets and contourlets (but not wavelets) yield $\alpha = 1$.

The reconstruction error results are presented in Table 1. CS(1) refers to the basic piecewise constant class and CS(2) refers to the subclass with smoother boundaries. We assume that CS employs an optimal basis or representation for reconstruction in each case (e.g., wavelet in CS(1) and curvelet in CS(2)). We see that in half of the situations considered, CS offers no advantage. When the SNR is high (close to noiseless situation) or when the boundary is sufficiently smooth, CS provides in improvement in the reconstruction error rate over what is possible using any pixel sampling scheme. It is our experience that most "real-world" images exhibit an approximation decay like $\alpha = 1/2$, and that rates approaching $\alpha = 1$ are relatively uncommon (apart from the simple images considered in our study). Thus, our analysis suggests that CS offers an advantage over conventional pixel sampling primarily in very high SNR imaging regimes.

6. SIMULATION EXPERIMENTS

To verify the that the theoretical bounds provide meaningful predictions in practice, we simulate the various schemes considered above. We compare the performance of pixel sam-

	Pixel Sampling	CS(1)	CS(2)
Noiseless	$k^{-1/2}$	k^{-1}	k^{-2}
Noisy	$k^{-1/2}$	$k^{-1/2}$	$k^{-2/3}$

Table 1. Reconstruction error bounds for different sampling schemes applied to piecewise constant images, assuming k observations and ignoring logarithmic factors.

pling to CS using Haar wavelet and wedgelet representations. For the wedglet-based reconstructions we use the code developed by Prof. Rebecca Willett [10], which we highly recommend, combined with the reconstruction algorithm described in [4]. The methods are evaluated in two settings, low-noise (SNR=9dB) and high-noise (SNR=3dB). The reconstruction error as a function of number of projections is plotted on log-log axes, for which power-law relationships yield linear relationships. The original signal, along with error plots for both noise settings are shown in Fig. 2. Note that our analysis focused on the decay rates, not constants, so attention should be paid solely to the slopes in Fig. 2. As predicted by the theory, the CS methods can sometimes outperform pixel sampling, especially at higher SNR. Further, using a reconstruction basis/representation that best approximates the class of images being considered (wedgelets in this case) provides even more of an advantage for CS.

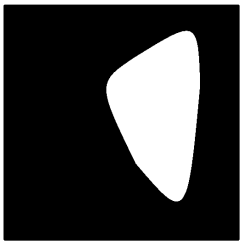

(a) Original Image

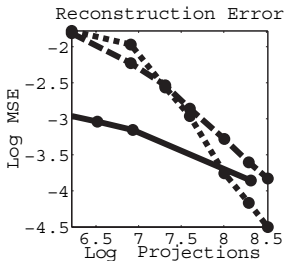

(b) 3dB Results

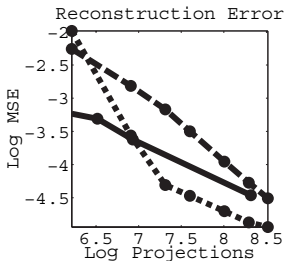

(c) 9dB Results

Fig. 2. Original Image and Reconstruction Errors. Pixel sampling error is shown with a solid line. The dashed line represents CS with a wavelet basis reconstruction, and the dotted line shows the error for CS with a wedgelet reconstruction.

7. CONCLUSIONS

We have shown that CS can be a useful imaging tool in various noise regimes when the underlying signal is compressible in a known basis or representation. However, many (perhaps most) "real-world" images exhibit an approximation error decay exponent close to $\alpha = 1/2$ and thus our analysis suggests that CS offers an advantage over conventional pixel sampling primarily in high SNR imaging regimes.

8. REFERENCES

[1] E. Candès, J. Romberg, and T. Tao, "Robust uncertainty principles: Exact signal reconstruction from highly incomplete frequency information," *IEEE Trans. Inform. Theory*, vol. 52, no. 2, pp. 489–509, Feb. 2006.

[2] E. Candès and T. Tao, "Near optimal signal recovery from random projections: Universal encoding strategies?," *IEEE Trans. Inform. Theory*, 2004, submitted.

[3] D. L. Donoho, "Compressed sensing," *IEEE Trans. Inform. Theory*, vol. 52, no. 4, pp. 1289–1306, April 2006.

[4] J. Haupt and R. Nowak, "Signal reconstruction from noisy random projections," *IEEE Trans. Inform. Theory*, 2005, to be published.

[5] E. Candès and T. Tao, "The Dantzig selector: statistical estimation when p is much larger than n," *Annals of Statistics*, 2005, submitted.

[6] E. Candès and D. L. Dohono, "Curvelets: A surprisingly effective nonadaptive representation for objects with edges," in *Curves and Surface Fitting: Saint-Malo 1999*, Larry Schumaker et al., Ed. Vanderbilt University Press, Nashville, TN, 1999.

[7] R. Willett and R. Nowak, "Platelets: A multiscale approach for recovering edges and surfaces in photon-limited medical imaging," *IEEE Trans. Med. Imag.*, vol. 22, no. 3, 2003.

[8] D. L. Donoho, "Wedgelets: Nearly-minimax estimation of edges," *Annals of Statistics*, vol. 27, pp. 859–897, 1999.

[9] M. N. Do and M. Vetterli, "The contourlet transform: An efficient directional multiresolution image representation," *IEEE Trans. Image Processing*, vol. 14, no. 12, pp. 2091–2106, December 2005.

[10] R. Willett, "Coarse-to-fine wedgelet image reconstruction Matlab code," 2005, on-line at `www.ee.duke.edu/~willett/Research/CTF.html`.